

Supporting Information

Large Sized Graphene Oxide/Modified Tourmaline Nanoparticles Aerogel with Stable Honeycomb-like Structure for High-efficiency PM_{2.5} Capture

Shiyu Zhang,¹ Jun Sun,¹ Di Hu,¹ Chao Xiao,¹ Qiqi Zhuo,² Jianjun Wang,¹ Chuanxiang Qin,¹
and Lixing Dai¹

¹College of Chemistry, Chemical Engineering and Materials Science, Soochow University,
Suzhou, Jiangsu, 215123, People's Republic of China.

²College of Material Science & Engineering, Jiangsu University of Science and Technology,
Zhenjiang, Jiangsu, 212003, People's Republic of China

Corresponding author e-mail: dailixing@suda.edu.cn; qinchuanxiang@suda.edu.cn

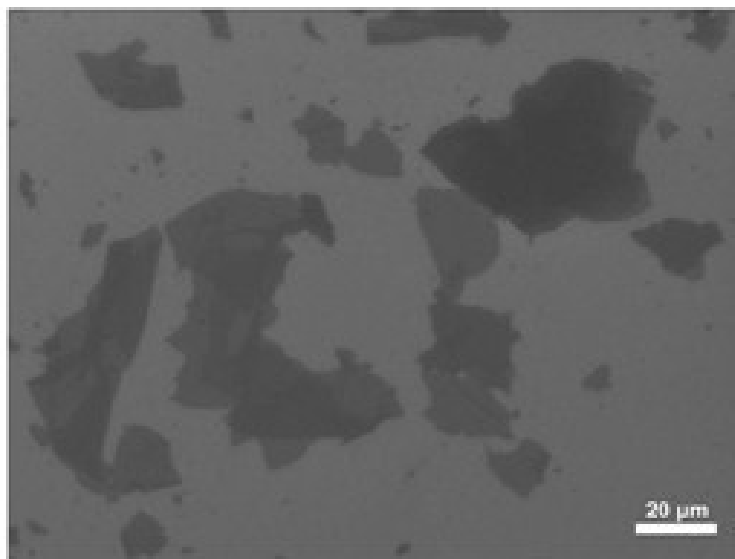


Figure S1. SEM image of LGO sheets used for preparation of aerogels. The sizes of LGO sheets are mostly (>97.6%) larger than $50 \mu\text{m}^2$.

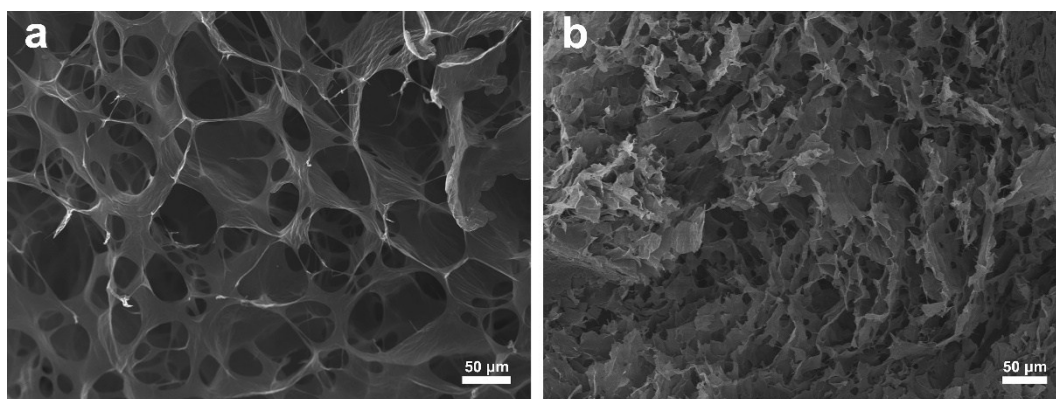


Figure S2. (a) SEM image of cross-section of LA. (b) SEM image of longitudinal section of LA.

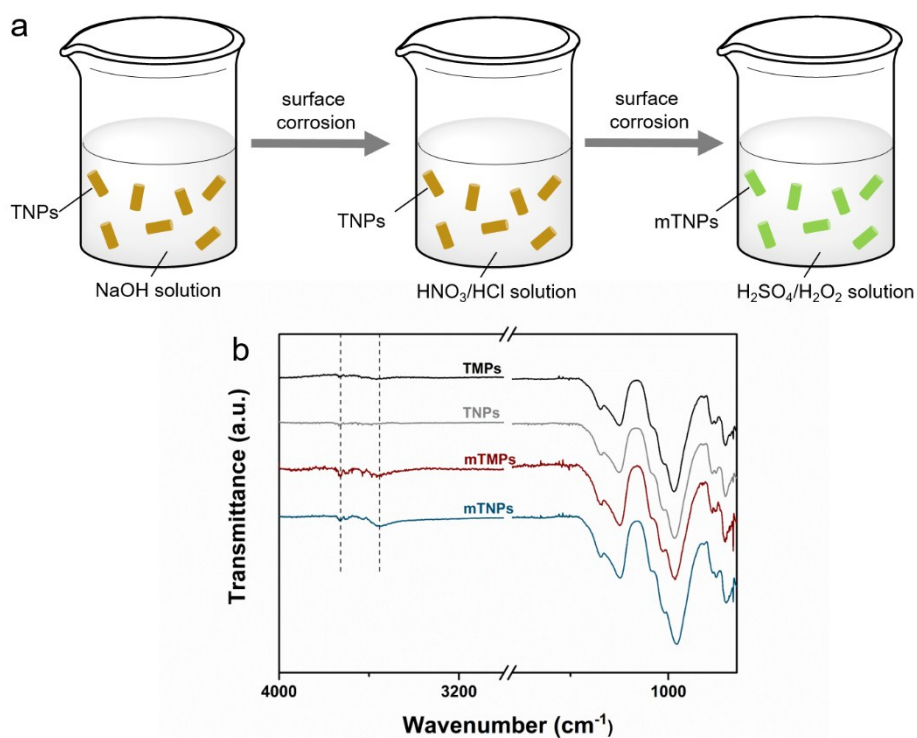


Figure S3. (a) Schematic of the processes for the modification of tourmaline with strong alkali, strong acid, and oxidants, respectively; (b) FTIR spectra of TNPs, mTNPs and mTNPs.

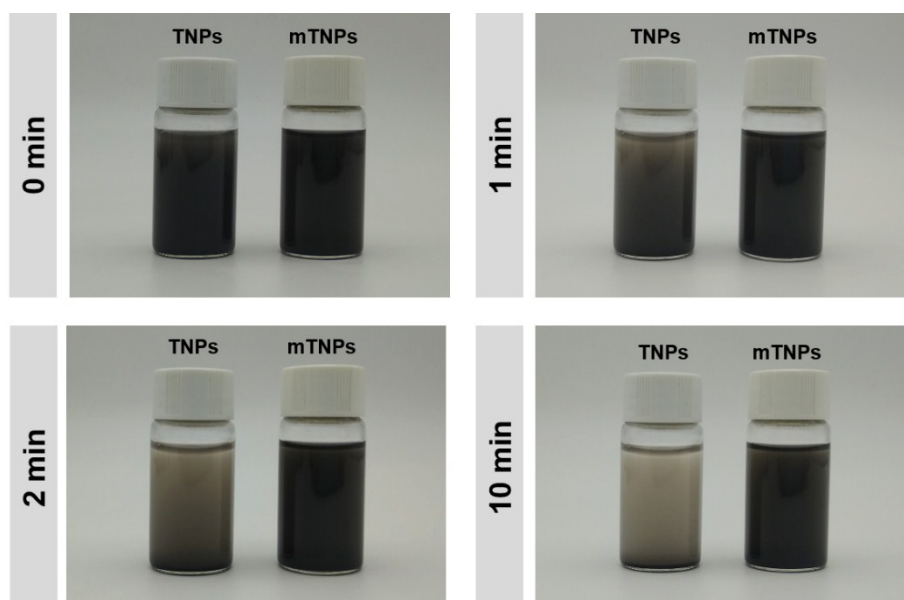


Figure S4. Digital photographs of TNPs and mTNPs aqueous dispersions at different staying time after sonication. The particle concentrations in the dispersions are $10 \mu\text{g mL}^{-1}$.

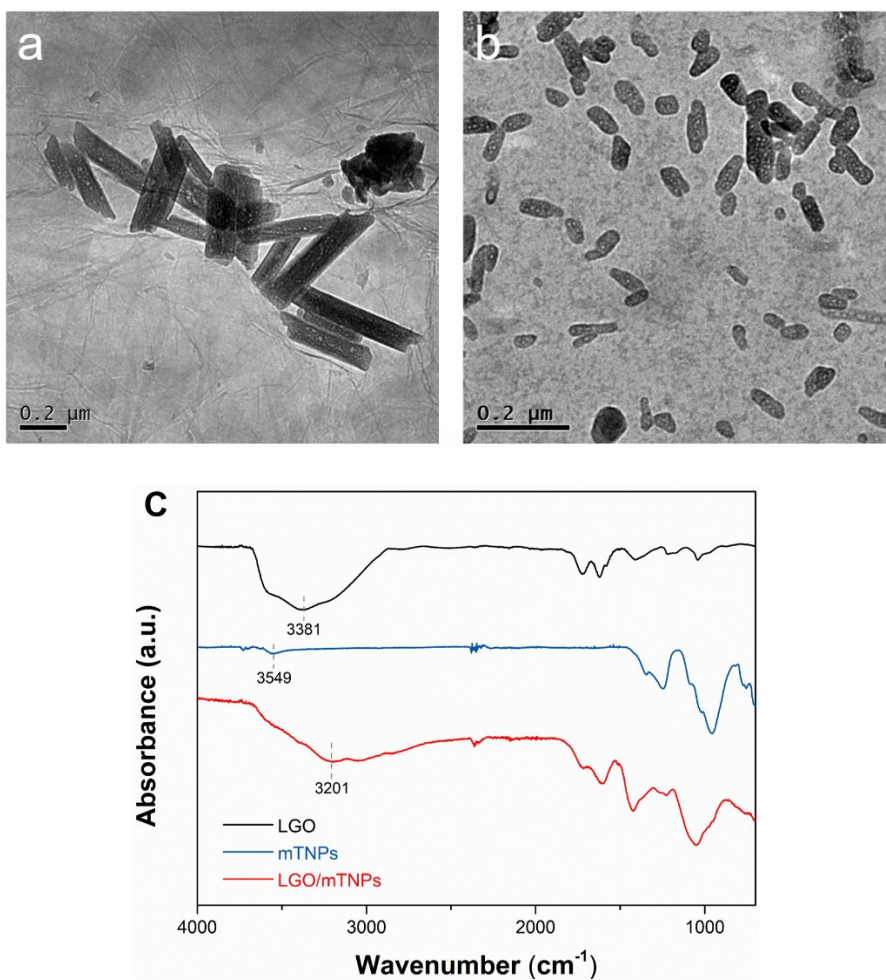


Figure S5. TEM images of TNPs (a) and mTNPs (b) distributed on LGO surface; (c) FTIR spectra of LGO, mTNPs and LGO/mTNPs(LTA5). That the sizes of mTNPs is much smaller than TNPs is caused by chemical corrosion during the modification.

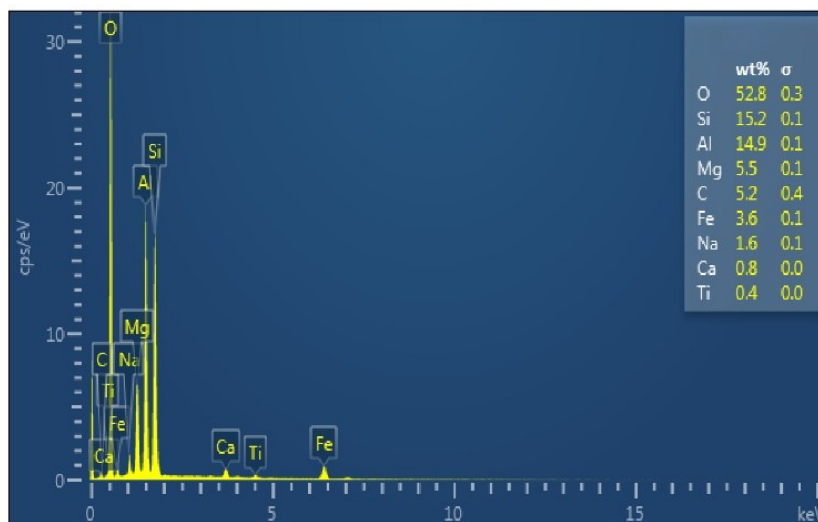


Figure S6. EDS spectra of mineral tourmaline. EDS curve indicates that mineral tourmaline contains elements such as oxygen, silicon, aluminum, magnesium, carbon, iron, and so on.

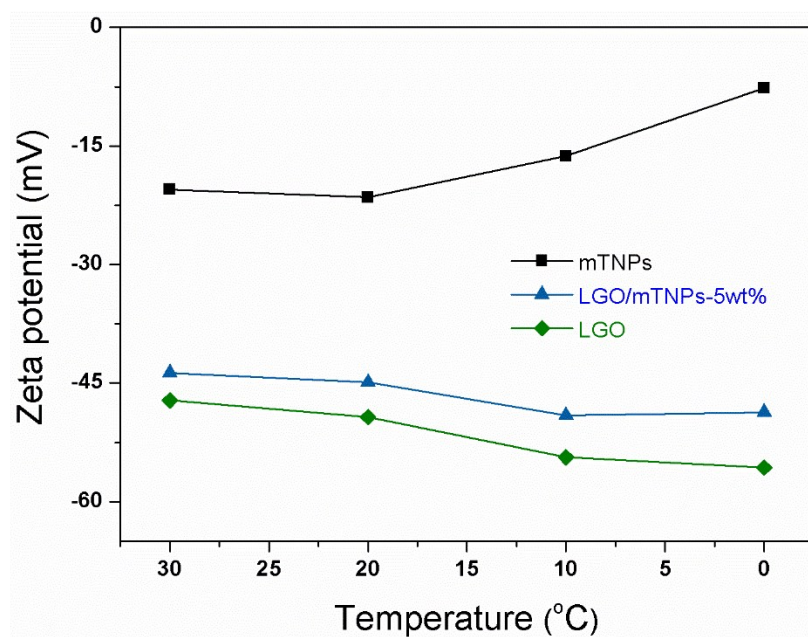


Figure S7. Zeta potential of mTNPs, LGO/mTNPs (mTNPs loading 5wt%) and LGO aqueous dispersions with different temperatures. Concentration for both LGO and LGO/mTNPs dispersions is 3 mg mL^{-1} , and concentration of mTNPs aqueous dispersion is 0.03 mg mL^{-1} .

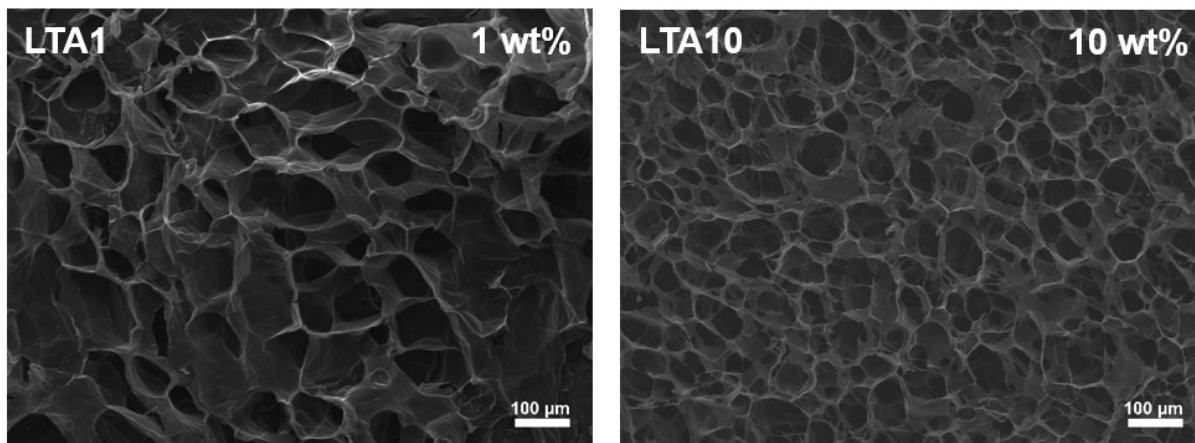


Figure S8. SEM images of cross-section of LTA1 and LTA10.

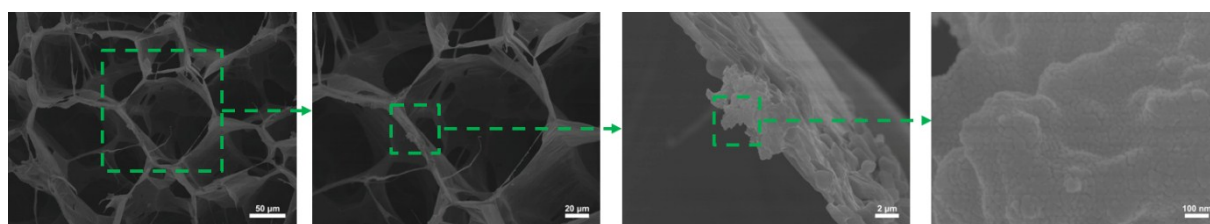


Figure S9. SEM images of LTA5 after PM_{2.5} capture test for 10 min. The magnification is gradually large from left to right. PM_{2.5} particles tend to aggregate on LGO sheets of LTA5.

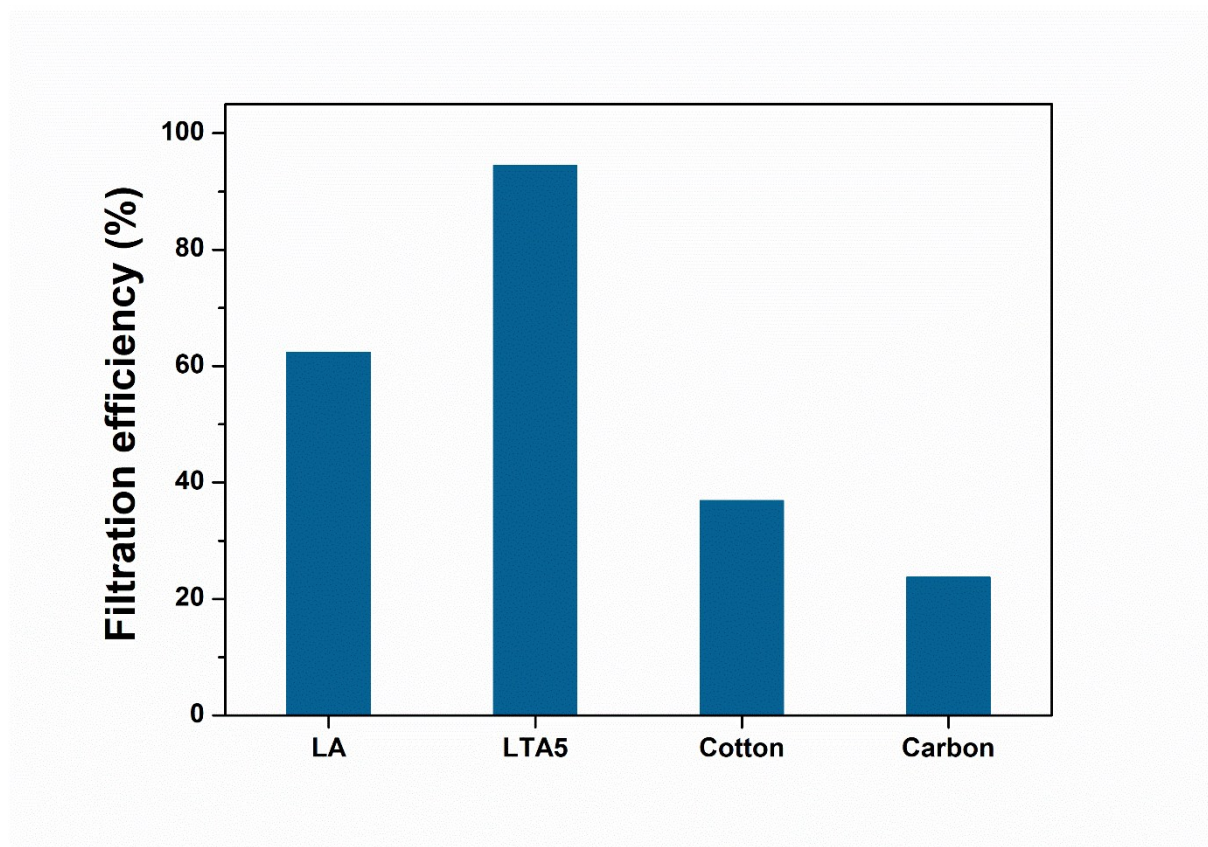


Figure S10. Filtration efficiency comparison for $PM_{2.5}$ among LA, LTA5, cotton and activated carbon with the same thickness 1mm.

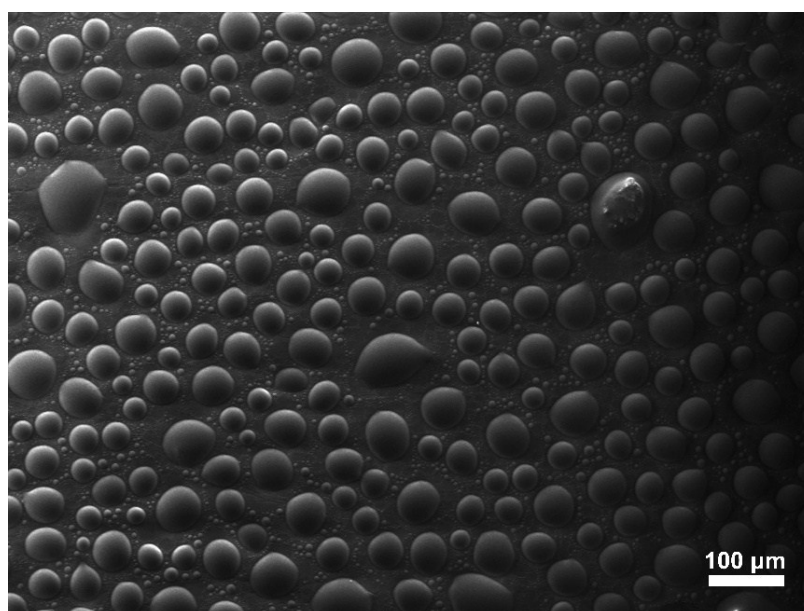


Figure S11. SEM image of aggregated droplet $PM_{2.5}$ on a silicon chip.

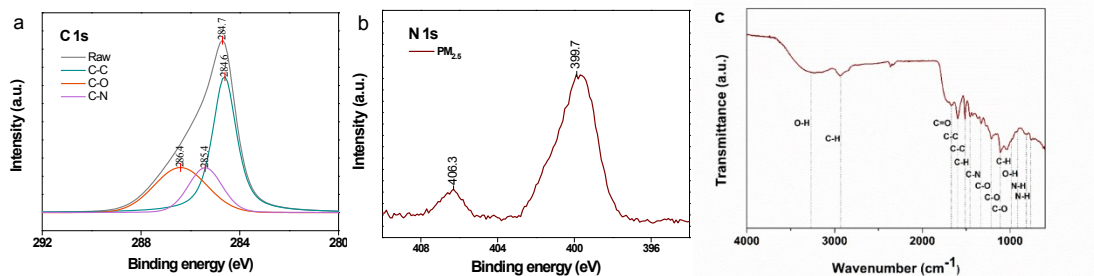


Figure S12. (a) C 1s XPS spectra of PM_{2.5}. (b) N 1s XPS spectra of PM_{2.5}. (c) FTIR spectra of PM_{2.5}. XPS only detected the surface chemical characteristics (about 5 nm in depth) of condensate PM_{2.5} collected on a silicon chip. In FTIR spectrum, the peaks appear at 3268.9, 2943.5, 1666.1, 1597.9, 1513.8, 1456.8, 1330.9, 1215.3, 1110.7, 1037.3, 984.8, 916.8, 807.1 and 765.3 cm⁻¹, manifesting the existence of C-C, C=C, C-H, C-N, N-H, O-H, C-O and C=O functional groups.

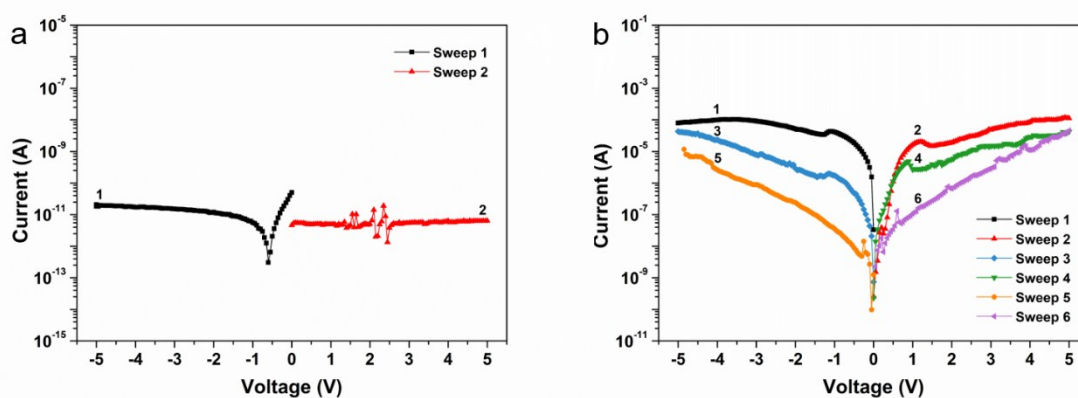


Figure S13. The electrical characteristics of LTA5 under long term idle state (a) and liquid nitrogen cooling state (b).